BNL-64728

CONF-970517--



# LATERAL INTERACTION ENERGY DERIVED FROM FRUMKIN ISOTHERM FOR C(2×2) Br/Ag(100)

J. X. Wang[1], T. Wandlowski[2], and B. M. Ocko[3]

[1]Chemical Science Division, Department of Applied Science
Brookhaven National Laboratory, Upton, NY 11973, USA
[2]Department of Electrochemistry, University of Ulm, D-89069 Ulm, Germany
[3]Department of Physics, Brookhaven National Laboratory, Upton, NY 11973, USA

## Abstract

The structure of the bromide adlayer on Ag(100) and the adsorption isotherm have been determined by using *in situ* surface x-ray scattering techniques and chronocoulometry. Bromide adsorbed on Ag(100) forms a fourfold-hollow-site lattice gas and the adsorption saturates at 1/2 monolayer in a $c(2 \times 2)$ structure. The Frumkin isotherm has been employed to fit the experimentally obtained isotherm, $\theta(E, C)$. Using the experimentally determined electrosorption valency, the lateral interaction energy of 220 meV/atom at full coverage is obtained.

## INTRODUCTION

Lateral interactions between adsorbates play an important role in determining adsorbate structure and phase behavior, including the isotherm. In electrochemistry, the Frumkin isotherm has been used to characterize the systems with repulsive or attractive lateral interactions (1). Unfortunately, the lack of structural information on adlayers has hindered investigations to develop atomistic views on the nature of lateral interaction in these systems. The advent of *in situ* scanning microscopic and surface x-ray scattering techniques has enabled the atomic structure at a single crystal electrode surface to be determined in great detail. Studies have shown that the structure of halide adlayer on Au and Ag electrodes depend considerably on the chemical nature of adsorbate, substrate as well as crystallographic orientation (2,3). Adsorption isotherms have been experimentally determined for several of these systems employing measurements of the "equilibrium" double layer capacitance (4) or more recently, chronocoulometry (5-7). Considerable difficulties still exist in deriving a microscopic understanding of the lateral interactions between adsorbed halide ions. In this paper, we present a semiquantitative attempt to model the nature of these interactions. Our approach is based on a Frumkin isotherm, and combines complementary results of *in situ* surface x-ray scattering and chronocoulometric experiments.

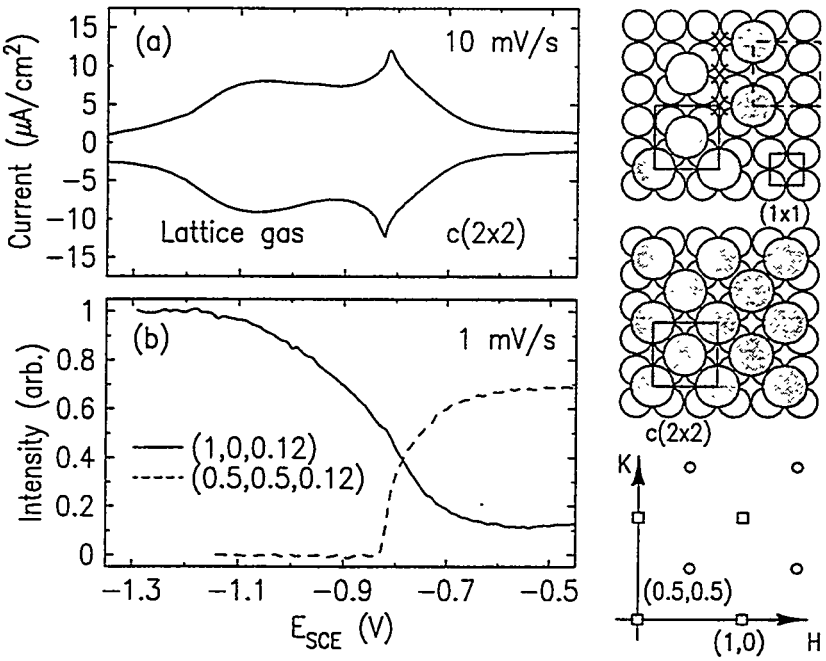


Figure 1: (a) Cyclic voltammogram for Ag(100) in 10 mM KBr and 40 mM $KClO_4$. (b) Diffuse scattering background subtracted x-ray intensities as a function of potential. Right panel: Real space sketch of the Ag(100) surface (open circles) and bromide (filled circles) adsorbed in the fourfold hollow sites in two anti-phase domains at low coverages (top) and a single domain of $c(2 \times 2)$ Br adlayer at full coverage (middle). The bottom part shows in-plane diffraction pattern observed from the Ag(100) substrate (squares) and the $c(2 \times 2)$ Br adlayer (circles).

## STRUCTURAL PHASE BEHAVIOR

Here we describe the results of our in-situ surface x-ray scattering measurements for Br on Ag(100) versus potential. For Ag(100) we use a body-centered-tetragonal unit cell with $a = b = 2.889$ Å (within the surface plane) and $c = 4.086$ Å (along the surface normal direction). Grazing incident angle diffraction measurements were carried out at $L = 0.12$.

As indicated by the cyclic voltammogram in Fig. 1a, bromide adsorption takes place over a wide potential region. Two peaks were found, a broad feature at negative potentials and a rather sharp peak ($\sim -0.83$ V) at more positive potentials. Below the sharp peak, in-plane diffractions are observed only at integer positions, which indicates the absence of a bromide superlattice. Above the peak potential additional diffractions were found at (1/2,1/2), (3/2,1/2), (5/2,1/2), and (3/2,3/2). This diffraction pattern corresponds to a $c(2 \times 2)$ adlayer structure as illustrated in Fig. 1. The evolution of the adlayer is mapped out by measuring the potential dependence of the

## DISCLAIMER

diffraction intensity at the (1/2,1/2) position. The rapid increase in the intensity at about $-0.83$ V, see Fig. 1, corresponds to the formation of the $c(2\times 2)$ ordered phase. This transition corresponds to an order/disorder transition. A complete account of this transition will be given elsewhere (8).

The potential dependence of the x-ray intensity at the (1,0,$L$) positions provides information on the registration of the adlayer relative to the substrate. The decrease in intensity at (0,1,0.12) with increasing potential, shown as the solid line in Fig. 1b, occurs since the bromide scattering amplitude is out-of-phase with that of the substrate. This out-of-phase condition is established when bromide is adsorbed in fourfold hollow sites. In contrast, for the adsorption at atop sites the scattering amplitudes are in-phase and the intensity would increase with increasing coverage. For adsorption at bridge sites the average Br scattering is zero since there is an equal probability for adsorption at the (0,1/2) and (1/2,0) positions and the scattering amplitudes from the adatoms at these two positions cancel. Thus, the intensity would be independent of coverage.

The (1,0,0.12) intensity curve shown in Fig. 1b is background subtracted and normalized to unity in the absence of Br adsorption. Note that the normalized intensity changes prior to the formation of the $c(2\times 2)$ phase, and levels off at 0.11 in the potential region where the (1/2,1/2,0.12) intensity from the $c(2\times 2)$ phase saturates. This is in good agreement with the calculated value, 0.103, as obtained with the expression (9):

$$\frac{I(1,0,L)_{\theta_h}}{I(1,0,L)_0} = \left|1 - \theta_h \frac{f_{Br}}{f_{Ag}}(1+e^{-i\pi L})e^{i2\pi Lz/c}\right|^2, \qquad (1)$$

where the fraction of occupied hollow sites, $\theta_h$, is set to 0.5. Here $f_{Ag}$ and $f_{Br}$ represent the atomic form factors of Ag and Br, respectively, and the Ag-Br layer spacing, $z$, is 2.30 Å (8).

This indicates that the fraction of occupied hollow sites is very close to 0.5, consistent with the expectations of a perfectly ordered $c(2\times 2)$ Br adlayer. In addition, the width of the (1/2,1/2,0.12) diffraction peak is nearly resolution limited, corresponding to a correlation length of 3000 Å, at all potentials within the $c(2\times 2)$ phase. These facts suggest that adsorbed bromides are mobile at the Ag(100) surface, i.e., they can hop from one hollow site to another. If the adatoms were locked into the initial adsorption sites, light domain walls, i.e., extra unoccupied sites, would exist between the anti-phase domains, which would result in an average coverage, or $\theta_h$, smaller than 0.5. This is illustrated in the top right panel of Fig. 1. The inaccessible sites between the two anti-phase domains are marked by "x". The unit cell for the two domains are drawn by the solid and dashed lines. They differ by a translational shift of a half lattice constant in the horizontal direction, hence, diffract out-of-phase from each other. The anti-phase domains would weaken the superlattice diffraction and broaden the peak width. These are not the case in both vacuum study for Cl adsorption on Ag(100) (10) and our study of electrosorption of bromide and chloride on

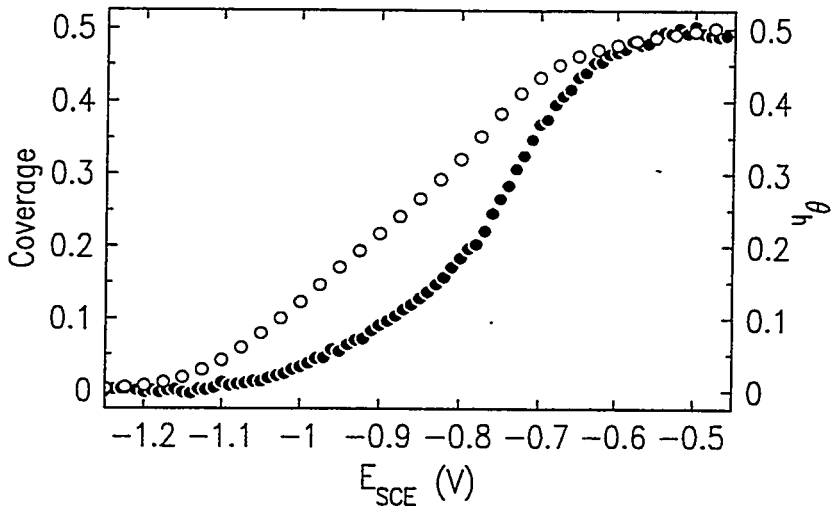


Figure 2: Atomic coverage of Br with respect to the Ag(100) surface (open circles) in 10 mM KBr obtained from chronocoulometry (left scale) and the fraction of the hollow sites occupied by Br (solid circles) as a function of potential (right scale).

Ag(100). In the former case, the sticking coefficient remains constant to within 0.05 monolayer of saturation (10) and in the latter, the hollow-site occupancy is within 10% of the saturation value for the $c(2 \times 2)$ structure.

Using Eq. 1, the fractional occupied hollow sites, $\theta_h$, as a function of potential is deduced and shown by the filled circles in Fig. 2. It is smaller than the Br coverage measured by chronocoulometry prior to saturation. The discrepancy indicates that even though the fourfold hollows are preferred, the Br adatoms are locked into the hollow sites only at high coverages. (We caution the reader that the atomic coverage with respect to the Ag(100) surface is used here which has a maximum value of 0.5 monolayer. In the following section, the fractional coverage which has been normalized to the maximum value is used in the isotherm analysis.) In summary, we have shown that bromide adsorbed on Ag(100) forms a square-lattice gas and the adsorption saturates at 1/2 monolayer in a $c(2 \times 2)$ structure.

## ADSORPTION ISOTHERM

For a simple charge transfer process, such as the formation of an adsorbed species A on a metal electrode, we write $A^Z + M + Ze^- \rightleftharpoons A\text{-}M$. The corresponding Frumkin isotherm can be expressed as (1)

$$\frac{\theta}{1-\theta} = K_0 C exp\left(\frac{-ZF(E-E_0)}{RT}\right) exp(-g\theta). \qquad (2)$$

where $\theta$ is the fractional coverage with respect to the maximum coverage, $K_0$ is the equilibrium constant, $C$ is the concentration of species $A^Z$ in the solution phase,

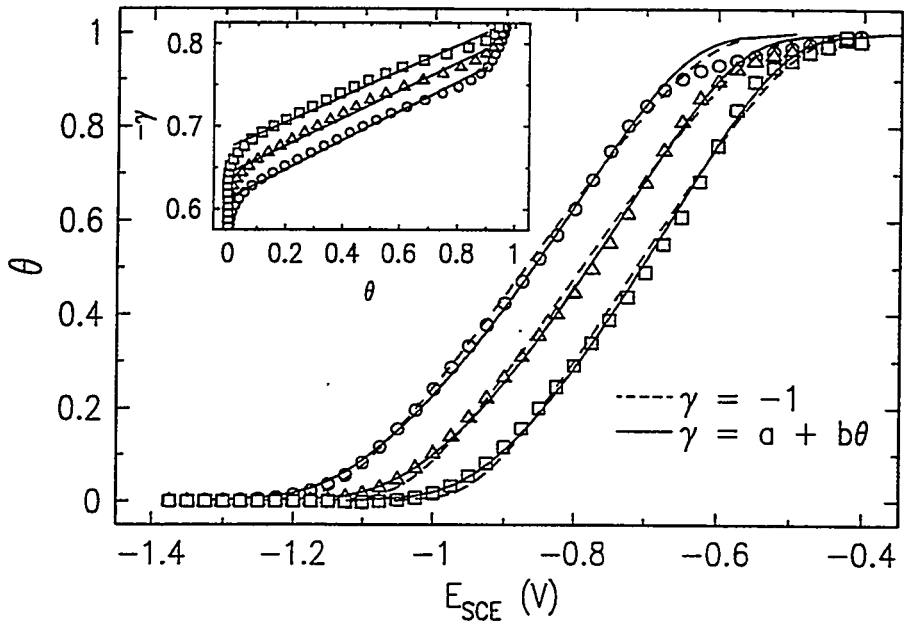


Figure 3: Potential dependence of the normalized Br coverage in 10 (circles), 1 (triangles), and 0.1 (squares) mM KBr + (50-$C_{KBr}$) mM $KClO_4$ solutions determined chronocoulometrically. Note that the normalized coverage is twice of the atomic coverage shown in Fig. 2. The dashed and solid lines are the fits described in the text. Insert: Electrosorption valency as a function of the Br coverage. The solid lines are the linear fits to the data.

and $E_0$ is an arbitrary reference potential. Eq. 2 represents the assumption that the lateral interaction energy, $gRT\theta$, depends linearly on coverage and that the adsorbate-substrate interaction is coverage independent. The dimensionless constant, $g$, is positive if the adsorbates repel, and negative if they attract each other.

When partial charge transfer occurs, the integral charge flow can be a fractional value between 0 and $Z$. This is described by the electrosorption valency, $\gamma$, which consists of contributions from the penetration of the substance into the double layer and the partial charge transfer (11). Parsons has shown that the Frumkin isotherm is equally applicable for any degree of charge transfer, provided that excess supporting electrolyte is used (12). The application to such a system, however, has not been demonstrated. By substituting $Z$ with $\gamma$, and $RTln(K_0)/F$ with $E_K$ in Eq. 2, the Frumkin isotherm can be written as

$$E = \left( \frac{RT}{F} (ln(\frac{\theta}{1-\theta}) - lnC + g\theta) - E_K \right) / (-\gamma) + E_0. \qquad (3)$$

Note that $E_K$ corresponds to the constant part of the adsorption energy which is independent of concentration and coverage, but may vary with the reference potential $E_0$.

For Br adsorption on Ag(100), $\theta = 1$ corresponds to the full coverage of a $c(2 \times 2)$ adlayer. This is equivalent to a coverage of 0.5 in terms of the number of fourfold hollow sites (see previous section). By using the normalized coverage (i.e., $\theta = \Gamma/\Gamma_{max}$) and the entropy term ($ln\frac{\theta}{1-\theta}$) in the Frumkin isotherm, we have assumed that each Br adatom effectively covers an area containing two hollow sites so that the number of the free sites decreases linearly with increasing coverage. If a lattice gas model is used, as shown by van der Eerden, the number of free sites decreases more rapidly than (1 - $\theta$) at low coverage and the entropy term has to be modified accordingly (13). Using this entropy term rather than $ln(\frac{\theta}{1-\theta})$, the fitted parameter $g$ decrease by about 5%. Despite this small difference, we have chosen to use the simpler "Frumkin type entropy term" in the following analysis.

A comprehensive thermodynamic analysis of chronocoulometrically acquired charge density and surface excess data for thirteen different KBr concentrations has been carried out and reported elsewhere (7). Fig. 3 shows the normalized Br coverage, $\theta$, as a function of potential for three KBr concentrations. The data within the 0.02-0.9 coverage region were first fitted with $\gamma = -1$ and $E_0 = -0.8$ V. The fits, as shown by the dashed lines, are reasonable. However, the two fitted parameters, $E_K$ and $g$ given in Table I (the third and fourth column, respectively), do not have the same value for the three concentrations. This is inconsistent with the definitions of $E_K$ and $g$, see Eq. 3, and can be corrected by using the experimentally determined electrosorption valency. The coverage dependent electrosorption valency, $\gamma(\theta)$, has been obtained from the potential dependent coverage, $\theta(E)$, and electrosorption valency, $\gamma(E)$. As shown in the inset of Fig. 3, $\gamma$ varies linearly with coverage over a wide region from the 0.02 to 0.9. The linear coefficients obtained from the fits are given in Table I (the sixth column). With $\gamma$ substituted by the corresponding linear equation, the fits (solid lines in Fig. 3) to the adsorption isotherms are slightly improved. More importantly, the $E_K$ and $g$ values (the seventh and eighth column in Table I) are nearly constant in these fits. Here the average value for $g$ is 8.55. Note, it is significantly smaller than that obtained with $\gamma = -1$. When $\gamma$ is kept at its average value, $-0.72$, the values of $g$ obtained from fitting are 9.48, 8.67, and 7.60 for KBr concentrations of 10, 1, and 0.1 mM, respectively. The average $g$ from these three concentrations, 8.85, is close to the value obtained from the fits with a coverage dependent $\gamma$. These results demonstrate a coupling between $\gamma$ and $g$ and suggest that the experimentally determined electrosorption valency should be used in analyzing adsorption isotherm.

In the Frumkin isotherm, the lateral interaction energy, $U$, is assumed to be zero at zero coverage and to increase linearly with coverage. This leads to

$$U = gRT\theta = 2.48g\theta \ (KJ/mol) \ at \ T = 298 \ K \tag{4}$$

or

$$U = gkT\theta = 25.69g\theta \ (meV/atom) \ at \ T = 298 \ K. \tag{5}$$

At full coverage, i.e., $\theta = 1$, the lateral interaction energy calculated from the $g$ value of 8.55 is thus equal to 21.2 KJ/mol or 220 meV/atom. Between zero and unity

Table 1: Parameters obtained from analysis of Br adsorption isotherm using Eq. 3 with $E_0 = 0.8$ V and $\gamma = -1$ or as a linear function of $\theta$, together with the mean square deviations ($\sigma^2$) of the fits.

| $C(mM)$ | $\gamma$ | $E_K(V)$ | $g$ | $\sigma^2(\times 10^4)$ | $\gamma$ | $E_K$(V) | $g$ | $\sigma^2(\times 10^4)$ |
|---|---|---|---|---|---|---|---|---|
| 10 | -1 | 0.39 | 15.28 | 0.9 | -0.62-0.18$\theta$ | 0.27 | 8.42 | 0.4 |
| 1 | -1 | 0.35 | 14.13 | 2.2 | -0.64-0.17$\theta$ | 0.27 | 8.68 | 0.4 |
| 0.1 | -1 | 0.31 | 12.62 | 3.9 | -0.67-0.16$\theta$ | 0.27 | 8.54 | 1.1 |

coverages, it assumes that $U$ is a linear function of $\theta$, independent of the adsorbate configuration. Even though this assumption seems to work, it may be fortuitous because of the cancellation of several effects. For instance, at low coverage, the adsorbed bromides are more charged but also further apart from each other. As the charge reduces at higher coverages, the average separation among the adsorbate also decreases. Their effects on the lateral repulsion energy may cancel each other out. In addition, a true microscopic model should also include the coverage-dependent indirect interaction as introduced by Einstein and Schrieffer (14). Finally, we note that the Frumkin model does not predict the observed order/disorder phase transition.

## LATERAL INTERACTION

For partially charged bromide adatoms, we assume here that the major lateral interactions can be described by the sum of Lennard-Jones (LJ) potential for a Br atom in neutral state and a dipole-dipole (dd) repulsion to account for the electrostatic interaction between the charges. The former includes the hard-core repulsion and Van der Waals attraction and is formulated as

$$u_{LJ} = 4\epsilon\left((\frac{\sigma}{r})^{12} - (\frac{\sigma}{r})^{6}\right), \tag{6}$$

where $r$ is the separation between a pair of Br adatoms, $\epsilon$ and $\sigma$ are the interaction parameters which have values of 12.76 meV and 3.7 Å, respectively (15). Assuming an image charge near the metal surface, the electrostatic interaction among the charged species on a metal can be described by the surface dipole interaction (16):

$$u_{dd} = \frac{\mu^2}{2\pi\epsilon_0 r^3}, \tag{7}$$

where $\mu$ is the surface dipole moment and $\epsilon_0$ is permittivity of free space. In this approach we do not incorporate screening effect of electrolyte and metal electrode surface.

The total lateral interaction energy per bromide in the $c(2\times 2)$ phase, $U$, can then be calculated by the summation of the pair interactions for the adatom at the (0,0)

position with all others at the (i,j) lattice sites:

$$U = \frac{1}{2}\sum_{i\neq 0}^{\infty}\sum_{j\neq 0}^{\infty}(u_{LJ}(r_{i,j}) + u_{dd}(r_{i,j})), \tag{8}$$

where the factor of $1/2$ is included to avoid the double counting of the pair interaction for calculating the energy per atom. The separation, $r_{i,j} = (i^2 + j^2)^{1/2}R$, where $R$ is the nearest neighbor separation of Br at the surface. Thus,

$$U = U_{LJ} + U_{dd} = 2\epsilon[(C_{12}(\frac{\sigma}{R})^{12} - C_6(\frac{\sigma}{R})^6] + C_3\frac{\mu^2}{4\pi\epsilon_0 R^3}, \tag{9}$$

where $U_{LJ}$ and $U_{dd}$ denote the total energy from Lennard-Jones potential and dipole-dipole interactions, respectively, and

$$C_m = \sum_{i\neq 0}^{\infty}\sum_{j\neq 0}^{\infty}(i^2 + j^2)^{-m/2}, \tag{10}$$

which gives 4.0640, 4.6565, and 8.977 for $C_{12}$, $C_6$, and $C_3$, respectively.

Using the Lennard-Jones parameters from ref. (15), $\sigma = 3.7$ Å and $\epsilon = 12.76$ meV the interaction, $U_{LJ}$, is very repulsive (1495 meV) at $R = 2.889$ Å and attractive ($-34$ meV) at $R = 4.086$ Å. These results show that the hard-core repulsion plays a major role in the exclusion of adsorption at the nearest neighbor hollow sites, but the repulsive energy in the $c(2 \times 2)$ phase must originate from electrostatic interaction. Since $U_{LJ}$ is $-34$ meV for the $c(2 \times 2)$ Br adlayer, a repulsive energy of 254 meV (i.e., $220 - (-34)$) is needed to account for the observed adsorption isotherm. According to Eq. 9, this corresponds to a dipole moment of 1.76 Debye. This value can only serve as an effective dipole moment for characterizing the system because the model oversimplifies the electrostatic interaction in an adlayer on a metal surface. The analysis, however, is useful for understanding the nature of the lateral interaction in halide adlayers on Ag(100). We have found that Cl adsorption on Ag(100) exhibits similar structural phase behavior as Br, but its adsorption isotherm, $\theta(E)$, is considerably sharper. This implies the lateral interaction is less repulsive or the electrosortion valency is closer to $-1$ for Cl than that for Br. At the first glance, the size seems to be the reason for Cl being less repulsive. It turns out to be incorrect because at the nearest neighbor separation, 4.086 Å, $U_{LJ}$ is attractive for both Br and Cl. The calculation of $U_{LJ}$ for Cl with $\sigma = 3.5$ Å and $\epsilon = 9.57$ meV (9), yields $-26$ meV. The values of $U_{LJ}$ for Cl and Br in the $c(2 \times 2)$ phase on Ag(100) are nearly the same. Therefore, the partial charge or the polarizability of the halide, rather than the atomic size, is the dominating factor in determining the lateral interaction energy, and hence its adsorption isotherm on Ag(100).

ACKNOWLEDGEMENTS

The authors thank S. Feldberg and R. R. Adžić for useful discussions. This research was performed under the auspices of the US Department of Energy, Division of Chemical and Material Sciences, office of Basic Energy Sciences under Contract No. DE-AC02-76CH00016, and financially supported by the Deutsche Forschungsgemeinshaft through a Heisenberg fellowship (T.W.) and a NATO CR Grant (T.W.).

REFERENCES

1. E. Gileadi, Electrode Kinetics, VCH Publishers, Inc., New York (1993).
2. B. M. Ocko, O. M. Magnussen, J. X. Wang, R. R. Adzic, Th. Wandlowski, Physica B **221**, 238 (1996).
3. A. A. Gewirth, B. U. Niece, Chem. Rev., **97**, 1129 (1997).
4. G. Valette, A. Hamelin, R. Parsons, Z. Phys. Chem. NF, **113**, 47 (1978).
5. Z. Shi, J. Lipkowski, J. Electroanal. Chem., **403**, 225 (1996), Z. Shi, J. Lipkowski, S. Mirwald, B. Pettinger, J. Chem. Soc. Faraday Trans. **92**, 3737 (1996).
6. M. L. Foriesti, G. Aluisi, M. Innocenti, H. Uobayashi, R. Guidelli, Surf. Sci., **335**, 247, 1995.
7. T. Wandlowski, J. X. Wang, B. M. Ocko, in preparation.
8. B. M. Ocko, J. X. Wang, and T. Wandlowski, Phys. Rev. Lett., in press.
9. H. L. Meyerheim, J. Wever, V. Jahns, W. Moritz, P. J. Eng, and I. K. Robinson, Surf. Sci. **304**, 267 (1994).
10. D. E. Taylor, E. D. Williams, R. L. Park, N. C. Bartelt, and T. L. Einstein, Phys. Rev. B. **32**, 4653, (1985).
11. J. W. Schultze, U. J. Velter, J. Electroanal. Chem. **44**, 63 (1973).
12. R. Parsons, J. Electroanal. Chem. **376**, 15 (1994).
13. J. P. van der Eerden, G. Staikov, D. Kashchiev, W. J. Lorenz, E. Budevski, Surf. Sci. **82**, 364 (1979).
14. T. L. Einstein and J. R. Schrieffer, Phys. Rev. B, **7**, 3629 (1973).
15. D. Scharf, K. Laasonen, Chem, Phys. Lett. **258**, 276 (1996).
16. W. Kohn and K.-H. Lau, Solid State Communication **18**, 553 (1976).